

New Approach To Study The Influence Of The Defect Structure On The Refractive Indices Of Mg-Doped Lithium Niobate

K. Maaider¹; A. Jennane^{1,2}; N. Masai^{1,2} and A. Khalil¹

¹ Laboratoire Rayonnement & Matière-Equipe de Recherche Physique de la Matière et Modélisation Université Hassan I^{er}, Faculté des Sciences et Techniques BP 577 Settat, Morocco

² Université Hassan I^{er}, Ecole Nationale des Sciences Appliquées BP 77 Khouribga, Morocco

Abstract: We proposed a new approach to calculate the refractive indices of Mg-doped lithium niobate using generalized vacancy models combined with a ferroelectric phase transition theory. We have obtained a generalised Sellmeier equation which takes into account the defect structure and Mg-doped lithium niobate. A comparison between the calculated values from this approach and the experimental data of the temperature and refractive indices is detailed.

I. Introduction

In these ferroelectrics, metal ions are incorporated mostly on Li-sites with a slight displacement from the original Li-positions^{1,2}. The requirement of charge compensation favors certain lattice environments for which different dopants are competing with each other. Once these sites are used up, other lattice sites are occupied by the dopants. For this reason, it is observed that some defects also occupy the Nb or the Ta-sites in particular, for higher doping levels and under co-doping with high levels of Zn [3, 4] and Mg⁵⁻⁸. LiNbO₃ single crystals of highest crystal quality can be grown from the congruent melt ($\approx 48.4\%$ Li₂O) by the Czochralski technique^{9,10}. The fabrication of off-congruent LiNbO₃ by this technique turns out to be difficult due to the strong composition difference between the melt and crystal. The early work into LiNbO₃ quickly revealed that the LiNbO₃ structure accepted a wide variety of dopant cations. Undoped LiNbO₃ is composed of corner-linked LiNbO₃ octahedra, producing 3 different cation sites; Li-site, Nb-site and an intrinsic vacancy. A large degree of disorder on these sites is tolerated, giving rise to the wide composition region¹¹ and the easy acceptance of many dopants¹². Through the selection of a particular dopant, different effects can be produced in LiNbO₃ leading to a variety of potential applications, Fig. 1.

Lithium niobate has a high potential for optical applications. Usually they require material with a distinct index of refraction and are often hampered by the photorefractive effect, also known as optical damage¹³. Both the refractive indices and its sensitivity to light illumination are influenced by the crystal composition or – to be more specific – by the number of Nb antisites in the crystal¹⁴. Besides the techniques which improve the stoichiometry without any doping¹⁵⁻¹⁷, several dopants like Mg¹³, Zn¹⁸, In¹⁹ and Sc²⁰ are known to reduce the optical damage.

Here we present measurements of the refractive indices of LiNbO₃ in a wavelength range from 0,4 to 1,06 μm and from 0 to 7.1 mol% Mg for doped lithium niobate. In combination with literature data for the temperature dependence of the refractive index we are able to determine the parameters of a Sellmeier equation which is a function of the four independent parameters wavelength, temperature, Li content and Mg content.

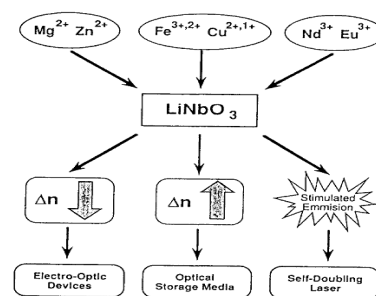


Fig. 1: Effect of different cation dopants on the optical properties of LiNbO₃.

II. Experimental Results

II-1. Characteristics Of The Crystals

The refractive indices of LiNbO₃ and LiNbO₃:Mg were measured by an interferometric technique which uses a monochromatically illuminated Michelson-type interferometer²¹. In one arm of the interferometer the parallel-plate sample is rotated around an axis parallel to the c axis of the crystal and perpendicular to the incident beam, causing a rotation-angle-dependent shift in the optical path-length difference. The resulting interferogram is measured with a computer-controlled setup and is evaluated with appropriate numerical fit procedures, yielding an accuracy of about $\Delta n = 5 \times 10^{-4}$ for samples of good optical quality^{22,23}. Using a helium-neon laser tunable in the visible and infrared region or a mercury vapor lamp combined

with a 0.2m monochromator several wavelengths in the range from 400 to 1200nm are available. Polarizing the light parallel or perpendicular to the rotation axis makes it possible to measure the extraordinary and the ordinary refractive index, respectively.

G. Kh. Kitaeva et al.²⁴ They used bulk Mg:LiNbO single crystals, grown by the Czochralski method. The starting material was close to congruently melting composition with the ratio Li/Nb=0.942²⁵. The MgO doping concentration varied from 0 to about 7 mol% under growth of different samples. The final concentration and spatial distribution of Mg in the grown crystals was studied by means of the fluorescent x-ray spectral analysis and wave dispersive x-ray microanalysis. The spatial variation of Mg-concentration in the samples was within ± 0.01 –0.03 mol%. The measurements of distribution of the impurity concentration within each crystal were made by x-ray microanalysis using Camebax SX-50 with a high relative accuracy. However, an absolute error of the value of an average Mg concentration was sufficiently larger, and exceeded 0.4 mol% for one of the crystals (see Table I).²⁴

Tab. 1 : Parameters of bulk Mg : LiNbO3 crystals

No.	Molar concentration of Mg(%)	Reduction conditions	The angle of second-harmonic generation 1.06 μm \rightarrow 0.532 μm , degrees
1	0	-	
2	4.4 \pm 0.1	-	75.9
2.1	4.4 \pm 0.1	at 500 °C, $P=10^{-5}$ Torr	
3	5.1 \pm 0.1	-	77.5
4	5.7 \pm 0.4	-	82.1
5	6.1 \pm 0.2	-	82.8
6	7.1 \pm 0.2	-	85.8
6.1	7.1 \pm 0.2	at 600 °C, $P=10^{-5}$ Torr	

Triangular prisms were cut for refractive index measurements in the visible range. The input and output polished surfaces of each prism were oriented along the crystal C axis, with an angle of $\sim 30^\circ$ between them. For measurements of absorption and refractive indices in the IR range, the samples were cut in the form of rectangular parallelepipeds. Input and output polished surfaces were also oriented along C axis. Absorption measurements were carried out in the samples of different thicknesses. The sample of the smallest thickness 8 μm was prepared by polishing of the undoped LiNbO. It was enclosed between two polished plates of the crystal BaF₂.

II-2. Refractive Index Dispersion

G. Kh. Kitaeva et al.²⁴ have measured the dispersion characteristics of ordinary (n_o) and extraordinary (n_e) refractive indices of the crystals in the visible range at

room temperature by the prism method, using a goniospectrometer. The absolute error did not exceed ± 0.0002 . Refractive indices at 1.06 μm were measured with the help of an image-converting visualiser. The obtained data in the region 0.4–1.06 μm were fitted by Sellmeier-type equations with coefficients differing for the differently doped samples²⁶. In this form they were used in subsequent measurements of the ordinary refractive indices in the IR range, made by two nonlinear-optical methods (Table II).

In the region of 1–1.25 μm the values of n_o were determined by measuring of the angle for second harmonic generation of a yttrium aluminum garnet (YAG):Nd laser and of a tunable LiF:F₂ laser. To calculate the $n_o(\lambda)$ values, the results for $n_e(\lambda/2)$ in the visible region were taken into account. They²⁴ estimate the total absolute error of the obtained data as ± 0.0005 . In the region of 2–5 μm the values of $n_o(\lambda)$ were obtained by spontaneous parametric light scattering (the down conversion) method. The optical scheme²⁶ included an Ar laser as a pump source at 0.488 nm. The pump wave was polarized extraordinarily, and the visible signal and IR idle waves were polarized ordinarily. The experimental values of indices ordinary represented in Tab. 1.

Concerning the variation of LiNbO defect structure under Mg doping, most models^{27,28,29,30,31-32} agree that there is a threshold in Md concentration, above which the crystal structure and properties change qualitatively. Above this threshold concentration C_{thr} , all defect atoms of Nb in Li antisites (NbLi) are replaced by Mg.³¹ the crystal becomes optically resistant and loses most of its photorefractivity.³³

Tab. II: Measured of n_o as a function of wavelengths λ in Mg:LiNbO3 crystals for different Mg concentrations.

Wavelength (nm)	Molar concentration of Mg(%)					
	0	4.4 \pm 0.1	5.1 \pm 0.1	5.7 \pm 0.4	6.1 \pm 0.2	7.1 \pm 0.2
1.064		2.2281	2.2277	2.2250	2.2231	2.2222
1.1334	2.229	2.2244	2.2238	2.2216	2.2193	2.2183
1.246	2.2206					
2.124	2.1937	2.1910	2.1841	2.1805	2.1798	2.1810
2.241	2.1869	2.1831	2.1807	2.1769	2.1752	2.1769
2.348	2.1825	2.1827	2.1772	2.1732	2.1713	2.1737
2.596	2.1710	2.1731	2.1659	2.1619	2.1625	2.1627
2.802	2.1593	2.1643	2.1582	2.1545	2.1525	2.1534
3.050	2.1471	2.1482	2.1482	2.1423	2.1413	2.1409
3.359	2.1341	2.1335	2.1336	2.1265	2.1244	2.1269
3.759	2.1097	2.1158	2.1127	2.1061	2.1013	2.1053
4.296	2.069	2.074	2.078	2.070	2.065	2.069
4.927	2.018	2.018	2.033	2.018	2.010	2.015

III. THEORETICAL APPROACH

A theory of ferroelectric phase transition in the crystal LiNbO₃ has been performed to understand and predict the properties of this crystal³⁴. In this system, the

solution of the dynamic problem of the crystal planes system exhibits the existence of the "soft mode" at the ferroelectric transition. In this work, we suppose that ceramic samples of LiNbO_3 are single crystal. Such an assumption is based on the experimental fact that the ferroelectric phase transition occurred in the ceramic samples which are formed by parallel planes along the polar "c" axis. In Figure 2, distances between planes (Li, Nb and O at $T=0$ K) are denoted as follow: $R_{\text{O-O}}(b=2.31\text{\AA})$, $R_{\text{Li-O}}(R_{20}=0.68\text{\AA})$, $R_{\text{Nb-O}}(R_{10}=0.883\text{\AA})$, $R_{\text{Li-Nb}}(R_{12}=b-R_{10}-R_{20})$ ³⁵. We avoid the detail of the theory of ferroelectric transition in the crystal LiNbO_3 which is similar to that of reference³⁴ and only report the useful expressions in the reference³⁷, for study to $\text{Mg}:\text{LiNbO}_3$. At 0°K , the soft mode frequency, ω^2 , is proportional to the Curie temperature. Substituting ω^2 to obtain the following relation that allows to calculate the Curie temperature³⁷:

$$\frac{T^*}{T} = \frac{M_1^* + M_2^* + M_0^*}{M_1 + M_2 + M_0} \left(\frac{M_1 M_2 M_0}{M_1^* M_2^* M_0^*} \right) \left(\frac{P_1^*}{P_1} \right) \left(\frac{P_2}{P_2^*} \right) \quad (1)$$

with

$$P_1^* = 3q_0 R_{12}^2 - q_1^* R_{20}^2 - q_2^* R_{10}^2$$

$$P_2^* = \frac{(R_{20} R_{21})^2}{q_2^*} \left(\frac{1}{M_1} + \frac{1}{M_0} \right) + \frac{(R_{10} R_{21})^2}{q_1^*} \times \left(\frac{1}{M_2} + \frac{1}{M_0} \right) - \frac{(R_{10} R_{20})^2}{3q_0^*} \left(\frac{1}{M_1} + \frac{1}{M_2} \right)$$

Expression 1 allows to determinate the Curie temperatures of the vacancy models. The element X represents the nonstoichiometric compositions and X^* is the nonstoichiometric doped compositions respectively.

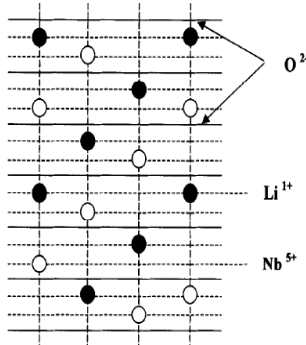


Fig. 2: Different planes in an elementary cell of crystal LiNbO_3 .

Refractive indices can be described by the Sellmeier equation:

$$n^2 = A_1 + \frac{A_2 + B_1 F}{\lambda^2 - (A_3 + B_2 F)^2} + B_3 F - A_4 \lambda^2$$

$$F = (T - 24.5) / (T + 570.5) \quad (2)$$

where λ is the wavelengths, T is the temperature (K) and A_i , B_i is the constants determinates. We introduce

the Refractive indices n^* , to explain the role of optical proprieties in nonstoichiometric doped $\text{Mg}:\text{LiNbO}_3$.

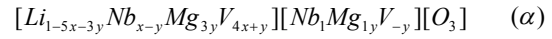
$$n^{*2} = A_1 + \frac{A_2 + B_1 F^*}{\lambda^2 - (A_3 + B_2 F^*)^2} + B_3 F^* - A_4 \lambda^2 \quad (3)$$

with X^* related to nonstoichiometric doped compositions. Although the expression of the T^* is determinate at Curie temperature point, this relation seems again correct to calculate the refractive indices about T^* .

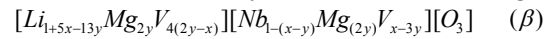
A comparative study between the calculated and measured values shows that the lithium vacancy model is the best model that has been suggested for describing the defect structure in nonstoichiometric lithium niobate. We assume the possible dominant Li-vacancy in the substitution process with C_{Mg} .

Taking into account of the experimental results, we have proposed the possible models:

- formula analyse before 3% mol of Mg:



- formula analyse after 3% mol of Mg:



In order to provide an adequate description of refractive indices in nonstoichiometric doped lithium niobate we have analytically performed the calculations of the Curie temperature as function of the composition x and the parameter y of the extrinsic concentration. Calculated and experimental³⁶ values of T^* for various nonstoichiometric compositions are illustrated in Figures 3.

The incorporation and substitution processes as function of C_{Mg} can be explain as follow: in the first stage, we certified that for the doping rate below 3%, it has an excess of niobium which can occupy the sites in the lithium vacancy model as deficient lithium in LiNbO_3 non-stoichiometric, like proposed by Masaif et al³⁷. In formulas where the doping rate is above 3%, we see that the dopant Mg is substituted in the two vacancy model cationic.

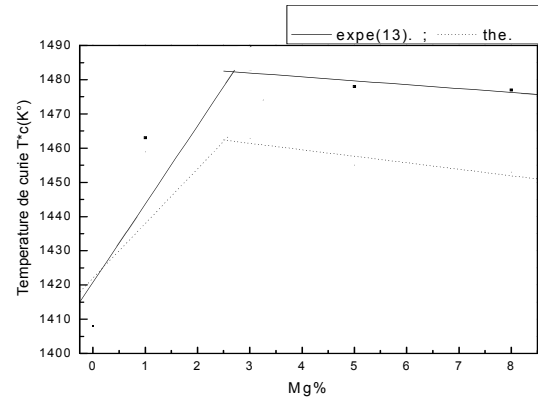


Fig. 3: Experimental and theoretical Evolution of the Temperature T^*c as a function of different rate of doping Mg.

IV. Results And Discussion

Doping LN solid solutions with magnesium, gives a explication from these models vacancy (α) and (β) for description of the structure of non-stoichiometric compound material LiNbO_3 doped with divalent magnesium, we have seen that the temperature also increases up to 3% and after lightly decrease, this will confirm that doping has two different mechanism, a 3% before and one after that rate. Calculated and experimental values of n^* for various

nonstoichiometric doped are illustrated in Figures 4. A comparison of the measured refractive indices with two vacancy models (before 3% and after 3% Mol:Mg) is indicate. According to experimental data, the refractive indices of LN compounds decreases with the increase of doping. In our work, we see that the refractive indices also decrease with the increase of Mg. We can say that these changes in properties of material are strongly related to the elimination of Nb ions in the lithium site, bay the substitution of foreign ions (Mg) in this site

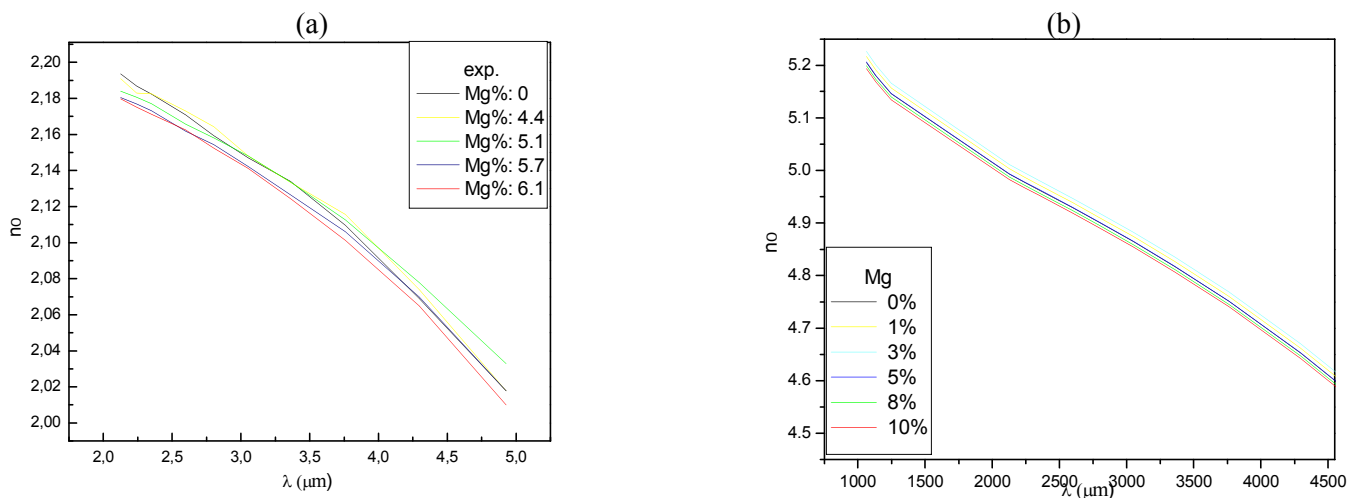


Fig. 4: Experimental (a) and theoretical (b) Evolution of n_o as a function of λ in the 0.4–1.06 μm range for LiNbO_3 with different rate of doping Mg.

V. Conclusion

In all this work, Vacancies play a fundamental role in the variation of the refractive indices, and we found much so that the intrinsic structure defect is well described by the model of deficient lithium. The experimental study shows that doping of LiNbO_3 crystals with magnesium lowers the optical damage. In our compounds, that is to say non-stoichiometric LN, application of the theory based on the structure simplified, combined with theoretical models vacancies (α) and (β), in refractive indices checked out the experience and serves to increase the resistance of optical damage.

In the experimental study, they were an extension of the Sellmeier equation, where this relationship requires some development, it is based on experimental measurements. We found that the combination approach with the classical equation of Sellmeier gives interesting results.

VI. References

- 1- Hauer, B., et al., Lattice site of Ti in LiNbO_3 , Journal of Physics Condensed Matter, 6, 1994.
- 2- Gog, T., et al., Lattice location of Ti and Er atoms in LiNbO_3 : An X-ray standing wave study, Ferroelectrics, 153, 1994.
- 3- Dierolf, V., et al., Comparative Studies of Er^{3+} ions in LiNbO_3 waveguides produced by different methods, Radiation Effects and Defects in Solids, 158, 2003.
- 4- Torchia, G. A., et al., Compositional effect on Cr^{3+} site distribution in MgO or ZnO codoped LiNbO_3 :Cr congruent and stoichiometric crystals, Journal of Physics Condensed Matter, 10, 1998.
- 5- Kling, A., et al., Lattice site determination of Cr in low doped lithium niobate single crystals using PIXE/channeling, Nuclear Instruments & Methods in Physics Research B, 136-138, 1998.
- 6- Malovichko, G., et al., Axial and low-symmetry centers of trivalent impurities in lithium niobate: Chromium in congruent and stoichiometric

- crystals, *Physical Review B (Condensed Matter)*, 59, 1999.
- 7- Boker, A., *et al.*, Two sites of Fe³⁺ in highly Mg-doped LiNbO₃, *Journal of Physics: Condensed Matter*, 2, 1990.
 - 8- Basun, S. A., *et al.*, Novel luminescent center in LiNbO₃:Cr:Mg crystals, *Journal of Luminescence*, 83-84, 1999.
 - 9- R. L. Byer, J. F. Young, and R. S. Feigelson, *J. Appl. Phys.* 41, 2320 (1970)
 - 10- P. F. Bordui, R. G. Norwood, C. D. Bird, and G. D. Galvert, *J. Cryst. Growth* 113, 61 (1991)
 - 11- P. Lerner, G. Legras and J. P. Dumas: *J. Cryst. Growth*, 3/4 (1968) 231.
 - 12- A. Rauber: *Current Topics in Materials Science* vol. 1, ed. E. Kaldis (North-Holland, (1978)
 - 13- D. A. Bryan, R. Gerson and H. E. Tomaschke, *Appl. Phys. Lett.* 44 (1984) 847.
 - 14- O. F. Schirmer, O. Thiemann and M. Wohlecke, *J. Phys. Chem. Solids* 52 (1991) 185.
 - 15- P. F. Bordui, R. G. Norwood, D. H. Jundt and M. M. Fejer, *J. Appl. Phys.* 71 (1992) 875.
 - 16- Y. Furukawa, M. Sato, K. Kitamura, Y. Yajima and M. Minakata, *J. Appl. Phys.* 72 (1992) 3250.
 - 17- G. I. Malovichko, V.G. Grachev, E.P Kokanyan, O.F. Shirmer, K. Betzler, B. Gather, F. Jermann, S. Klauer, U. Schalrb and M. Wohlecke, *Appl. Phys. A* 56 (1993) 103.
 - 18- T. R. Volk, V. I. Pryalkin and N. M. Rubinina, *Optics Lett.* 15 (1990) 996.
 - 19- T. R. Volk and N. M. Rubinina, *Ferroel. Lett.* 14 (1992) 37.
 - 20- J. K. Yamamoto, K. Kitamura, N. Iyi, S. Kimura, Y. Furukawa and M. Sato, *Appl. Lett.* 61 (1992) 2156.
 - 21- M. S. Shumate, *Appl. Opt.* 5, 327 (1966).
 - 22- K. Betzler, A. Grone, N. Shmildt, and P. Voigt, *Rev. Sci. Instrum.* 59, 652 (1988).
 - 23- U. Schlarb and K. Betzler, *Ferroelectrics* 126, 39 (1992).
 - 24- G. Kh. Kitaeva, K. A. Kuznetsov, A. N. Penin et A. V. Shepelev; *Physical Review B*, Vol 65, 054304 (2002)
 - 25- I. I. Naumova, *Crystallogr. Rep.* 39, 1029 (1994)
 - 26- G. K. Kitaeva, K. A. Kuznetsov, I. I. Naumova, and A. N. Penin, *Kvant. Electron. (Moscow)* 30, 726 (2000)[*Quantum Electron.* 30, 726 (2000)].
 - 27- T. Volk and M. Wohlecke, *Ferroelect. Rev.* 1, 195 (1998)
 - 28- O. F. Schirmer, O. Thiemann, and M. Wohlecke, *J. Phys. Chem. Solids* 52, 185 (1991)
 - 29- B. Faust, H. Muller, and O. F. Schirmer, *Ferroelectrics* 153, 297 (1994).
 - 30- T. Volk, N. Rubinina, and M. Wohlecke, *J. Opt. Soc. Am. B* 11, 1681 (1994).
 - 31- H. Donnerberg, S. M. Tomlinson, C. R. A. Catlow, and O. F. Schirmer, *Phys. Rev. B* 44, 4877 (1991).
 - 32- K. L. Sweeney, L. E. Halliburton, D. A. Bryan, R. R. Rice, R. Gerson, and H. E. Tomaschke, *J. Appl. Phys.* 57, 1036 (1985).
 - 33- D. A. Bryan, R. Gerson, and H. E. Tomaschke, *Appl. Phys. Lett.* 44, 847 (1984).
 - 34- F. P. Safaryan, *Physics Let. A*, 191 (1999) 255.
 - 35- N. Iyi, K. Kitavura, F. Izumi, I. K. Yamamoto, T. Hayashi, H. Asano, S. Kimura, *J. Sol. State chem.* 101 (1992) 340-352.
 - 36- T. Katsumata, K. Shibata and H. Imagawa, *Materials research bulletin*, Vol. 29, N°5, pp. 559-566 (1994)
 - 37- N. Masaif, S. Jebbari and A. Jennane, 8th International Conference on Condensed Matter and Statistical Physics, 8th ICCMSP – Marrakech – Abstract book, p. 69, 21-24 Septembre 2004.